

Optical and electrical properties of a squaraine dye in photovoltaic cells

Guo Chen,¹ Daisuke Yokoyama,^{1,a)} Hisahiro Sasabe,¹ Ziruo Hong,^{1,a)} Yang Yang,² and Junji Kido¹

¹Department of Organic Device Engineering, Graduate School of Engineering, and Research Center for Organic Electronics (ROEL), Yamagata University, Yonezawa, 992-8510, Japan

²Department of Materials Science and Engineering, University of California, Los Angeles, California 90095, USA

(Received 13 March 2012; accepted 8 August 2012; published online 23 August 2012)

2,4-Bis[4-(N,N-diisobutylamino)-2,6-dihydroxyphenyl] squaraine (SQ) was employed as a donor material in organic photovoltaic cells based on planar heterojunctions. We studied optical properties of SQ films, and discussed its photovoltaic performance via numerical fitting and simulation on the photovoltaic cells. Exciton diffusion length (L_D) in SQ films (4.5 nm) derived from optical simulation should be the major limitation to efficiency, consistent with external quantum efficiency data. Thermal treatment improved efficiency, which can be ascribed to reduced saturation current of the photovoltaic cells. As a result, a power conversion efficiency of 4.1% was achieved. © 2012 American Institute of Physics. [<http://dx.doi.org/10.1063/1.4747623>]

Among varied photovoltaic technologies, organic photovoltaic (OPV) is an attractive candidate for solar energy applications, because OPV cells can be processed on light-weight flexible substrates via low-cost large-area coating techniques.¹ Molecular structures and band gaps of organic compounds can be modified, so that efficient light harvesting throughout UV to infrared can be achieved. Power conversion efficiency (PCE) of organic solar cells is moving forward rapidly to 10%.^{2–8}

Both solution processes and thermal evaporation are used to fabricate OPV cells. Polymer and recently some low-molecular-weight materials are coated from solutions.⁹ For low-molecular-weight compounds, vacuum deposition is so far a good method to obtain high-quality films. Among these, 2,4-bis[4-(N,N-diisobutylamino)-2,6-dihydroxyphenyl] squaraine (SQ) has been demonstrated to be a good donor material with unique advantages.^{10,11} SQ and its analogs can be dissolved and processed via solution process.¹² Thermally deposited SQ/C₆₀ photovoltaic cells showed decent efficiency.¹⁰ That means SQ can be incorporated into various device architectures via various coating techniques. Squaraine compounds have extinction coefficients of as high as $\sim 3 \times 10^5 \text{ cm}^{-1}$. Therefore, ~ 10 -nm-thick squaraine films may cause significant absorption and photocurrent generation. Greater than 6% of PCE has been realized from SQ:fullerene heterojunctions.^{12,13} Solution processed squaraine films yield high OPV performance in combination with vacuum deposited fullerene layers.¹²

With continuously increasing photovoltaic performance, it is desirable to understand optical properties of SQ compounds and sequential effects on photovoltaic performance. In this work, we investigated optical properties of SQ films using ellipsometry. Based on that, optical simulation was carried out to understand photovoltaic performance in SQ/fullerene planar heterojunction devices. Short L_D was found to be the major limiting factor for PCE. Our finding shows that thermal

treatment enhanced PCE of $>4\%$, reaching state-of-the-art level in planar heterojunction based OPV cells. This is mainly attributed to reduction in saturation current (J_0).

SQ compound was in-house synthesized according to literature procedure.¹⁴ MoO₃, fullerene C₆₀ and C₇₀, and bathocuproine (BCP) were commercially available. All organic materials were purified by multi-step thermal sublimation. Indium-tin-oxide (ITO) coated glass substrates were cleaned by acetone, deionized water, and isopropanol in sonication, and treated in UV-ozone for 30 min before loading into a vacuum chamber. Organic and metal films were then sequentially deposited on top of ITO substrates via thermal evaporation at base pressure of 1×10^{-6} Pa. The device structure is ITO/MoO₃ (5 nm)/SQ (X nm, X = 6.5–18 nm)/C₆₀ or C₇₀ (40 nm)/BCP (8 nm)/Al (100 nm). 5 nm thick MoO₃ was inserted between SQ film and the ITO surface to form an ohmic contact for hole collection.¹⁵ Thickness of SQ layer was changed for device optimization and numerical simulation. Aluminum was deposited on top of the organic layers through a shadow mask, and the overlap between ITO anode and Al cathode defined an active area of $2 \times 2 \text{ mm}^2$. The made-up devices were transferred directly to a nitrogen-filled glovebox for encapsulation without exposure to air. External quantum efficiency (EQE) and current density-voltage (J-V) characteristics were measured on an integrated characterization system for thin film solar cells, CEP-2000 by Bunkoukeiki Co. Both AC with chopper frequency of 80 Hz and DC modes were used to ensure accurate EQE. PCE was obtained under 100 mW/cm^2 AM1.5G solar spectrum using a reference silicon diode with a KG-5 filter, calibrated by National Institute of Advanced Industrial Science and Technology in Japan. Integration of EQE with standard solar spectrum yields calculated short circuit current (J_{sc}) close to measured J_{sc} with less than 5% discrepancy. Absorption spectra were taken on a SHIMADZU MPC-2200 UV-Visible spectrophotometer. Highest occupied molecular orbital (HOMO) of SQ and fullerenes was determined using ultraviolet photoelectron yield spectroscopy by Sumitomo Heavy Industry PYS and Riken Keiki AC-3. The lowest unoccupied

^{a)}Authors to whom correspondence should be addressed. Electronic mail: d_yokoyama@yz.yamagata-u.ac.jp, ziruo@yz.yamagata-u.ac.jp.

molecular orbital (LUMO) was then derived by subtracting bandgaps from HOMO levels. Optical constants, i.e., refractive indices (n) and extinction coefficients (k) of 100-nm-thick organic layers, were determined by variable angle spectroscopic ellipsometer as described previously.¹⁶ Using these optical constants, we carried out numerical simulation to calculate absorption and EQE spectra of multilayer structures following the procedure of optical simulations,^{2,17} enabling us to investigate and discuss the light absorption and exciton diffusion in the OPV cells.

Fig. 1(a) shows molecular structures and absorption profiles of organic materials. Thickness of SQ film was varied from 6.5 nm to 18.0 nm for efficiency optimization. SQ film thickness of 6.5 nm delivers PCE of 2.7% with open circuit voltage (V_{oc}) of 0.79 V, J_{sc} of 5.7 mA/cm⁻², and fill factor (FF) of 59%, consistent with previous report.¹⁰ When thickness increased to 9.0 nm, there was little change with device performance, while data became more coherent and reliable. Therefore, we used 9.0-nm-thick SQ film in OPV cells.

Fig. 1(b) shows the optical constants of the SQ film. We found that SQ film showed slightly anisotropic property, because its linear molecular shape favors alignment in films on molecular level.¹⁸ k in the horizontal direction (k_o) is larger than that in the vertical direction (k_c), showing that the transition dipole moment of SQ molecules is slightly oriented in parallel to substrate surface. C₆₀ and BCP films have isotropic optical properties according to previous report.¹⁹ When evaluating PCE and EQE, the simulated solar light is a parallel beam perpendicular to the film plane.

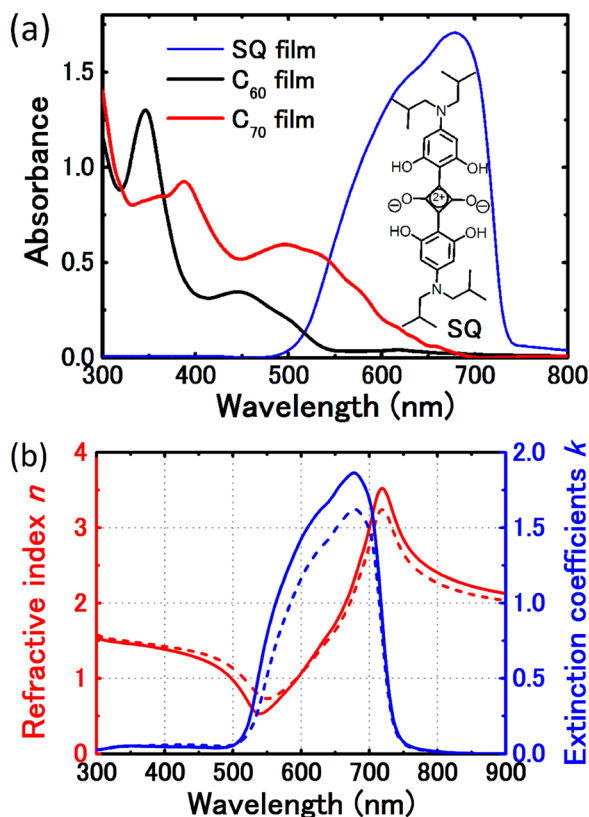


FIG. 1. (a) Molecular structure of SQ, and absorption of SQ, C₆₀, and C₇₀ films (100 nm); (b) optical constants of SQ films on Si substrate. (b) Optical parameters of SQ film, n_o (red solid), n_c (red dotted), k_o (blue solid), and k_c (blue dotted).

Therefore, we use n_o and k_o in the optical simulation, deriving L_D and calculating optical profiles and exciton distribution without taking any optical approximation.

In our simulation, efficiency for both exciton dissociation into free carrier and charge collection by electrodes is considered as 100%. Regarding exciton dissociation, we confirmed that photoluminescent (PL) emission from donor film is too weak to measure. Therefore, to make sure that the assumption is valid, we measured HOMO and LUMO levels of both donor and acceptor materials. HOMO and LUMO levels of SQ were 5.3 eV and 3.6 eV, respectively. Fullerene C₆₀ and C₇₀ have similar LUMO and HOMO levels of 4.2 eV and 6.1 eV. The data indicate sufficient energy level offset (>0.5 eV) for efficient charge transfer.

Regarding charge collection efficiency, it has been proved that the charge carriers can be swept out completely within thin film devices at reverse bias of -2 V as demonstrated by Blom's group.²⁰ According to our bright state J-V curves, the ratio of photocurrent (J_{ph}) at -2 V to J_{sc} , i.e., J_{ph} at 0 V, is ~1.08. Such a value suggests that charge collection efficiency at 0 V is well above 90%. With that, we are convinced to use charge collection efficiency of nearly unity in optical simulation.

Taking into account that exciton dissociation and charge collection are 100% efficient in OPV cells, EQE of a planar heterojunction is determined by optical constants of all layers, and L_D in the active layers, e.g., absorption efficiency and exciton collection efficiency. Thus, if EQE can be measured experimentally, and absorption profile in the thin film device can be calculated, we shall be able to calculate L_D in individual films. In Fig. 2(a), we show the experimental and simulated EQE spectra, from which the diffusion lengths in the SQ and C₆₀ layer of 4.5 nm and 23 nm, respectively, were derived. From this result, we can understand why the SQ layer in planar heterojunction based OPV cells should be thin such as 9 nm; this is because the diffusion length in the SQ layer is small. In spite of the small diffusion length of 4.5 nm, the OPV cells still delivered considerable J_{ph} due to the large extinction coefficient of the SQ layer due to the large oscillator strength of the SQ molecule itself. As for L_D in C₆₀ film, our calculated value is consistent with previous reports by Peumans and Forrest² and Cheyns *et al.*²¹

Fig. 2(b) shows the absorption profile distribution vs wavelength in the bilayer device. It is clear that the blue light is mainly absorbed in C₆₀ layer, and red and near infrared in SQ layer. The absorption maxima of both red and blue lights are close to the donor/acceptor interface, which facilitates exciton separation and charge generation. However, from the effective optical absorption profile shown in Fig. 2(c), the utilization of excitons in SQ layer is far less sufficient, and that suggests the huge potential of SQ to explore.

From SQ/C₆₀ heterojunction, we saw a deep dip in the EQE curve from SQ/C₆₀ heterojunction shown in Fig. 2(a), meaning insufficient green light capturing. Therefore, we use fullerene C₇₀ replacing C₆₀. Fig. 3(a) shows EQE curves of SQ/C₇₀ heterojunction cells. The average EQE value reaches over 30% throughout visible range, and thus J_{sc} of ~8.0 mA/cm² is observed, which is almost 30% higher than that from C₆₀ based devices. However, the FF of approximately 56% limits PCE in comparison with state-of-the-art bilayer organic photovoltaic cells.^{19,22,23}

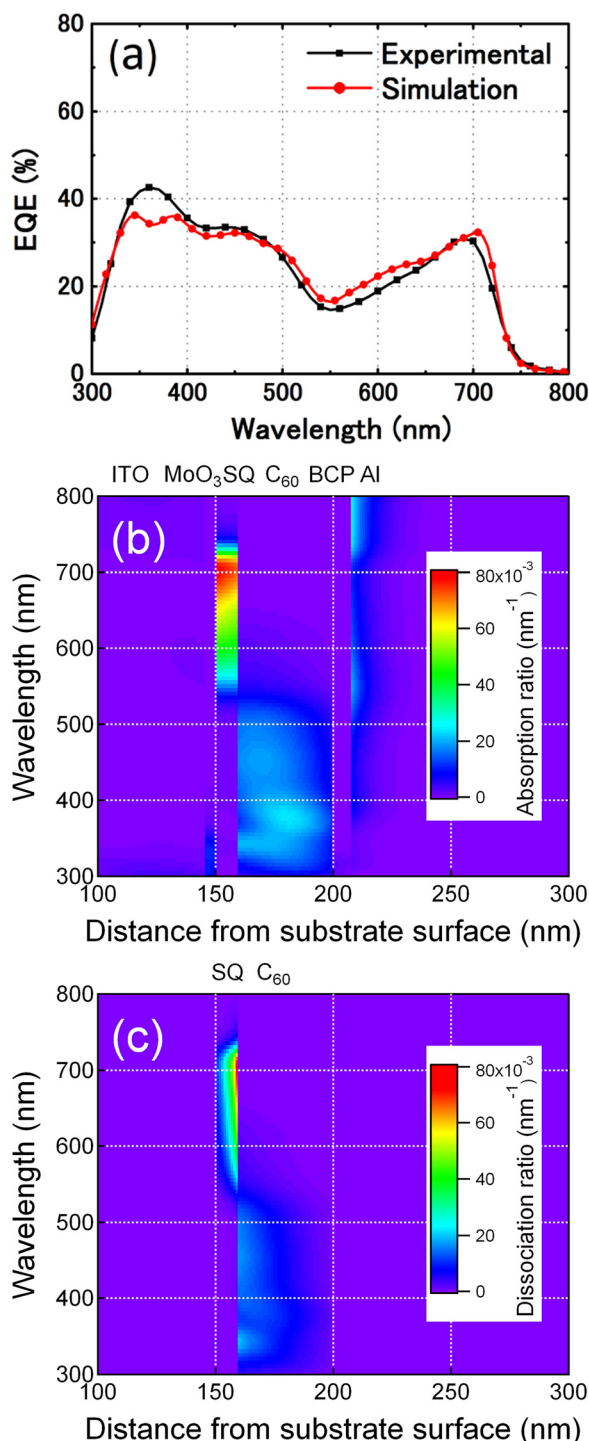


FIG. 2. (a) Experimental and simulated EQE spectra of SQ/C₆₀ bilayer OPV cells; (b) absorption profile, and (c) exciton distribution for effective charge generation.

Thermal treatment of photovoltaic cells at 90 °C for 4 min enhanced PCE. As shown in Fig. 3(b) and Table I, all three parameters with respect to PCE, i.e., J_{sc} , V_{oc} , and FF, were improved spontaneously. PCE from thermally treated cells reached 4.1%. Among them, FF was improved up to 63%. Though the serial resistance was kept almost the same according to the forward bias injection, the shunt resistance increased, which is responsible for improved FF. It suggests that reduced field dependent charge recombination occurs, which might be due to mobility increase in SQ film after thermal treatment.¹⁰ It is supported by the EQE profiles shown in

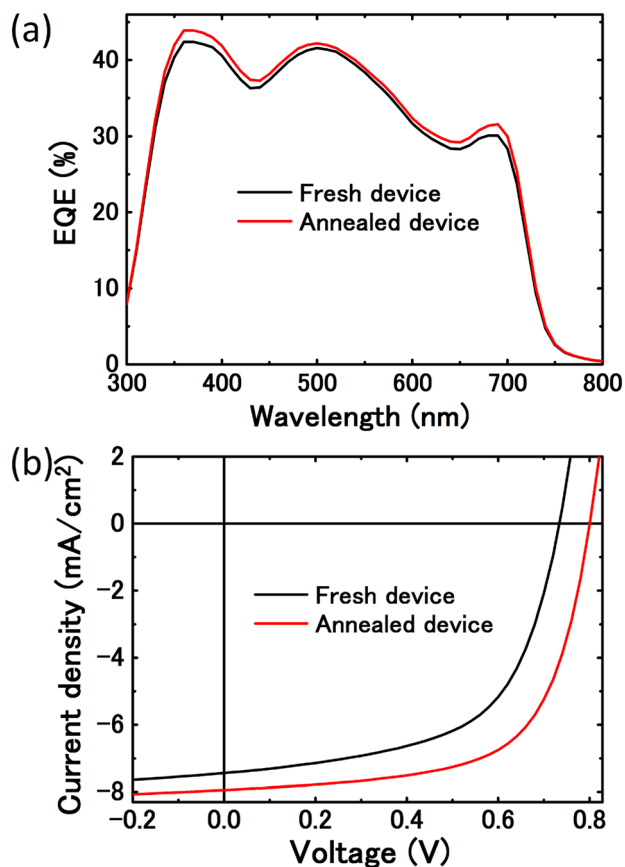


FIG. 3. (a) EQE spectra and (b) J-V characteristics illuminated at 100 mW/cm² (AM 1.5 G solar spectrum) for the SQ (9 nm)/C₇₀ (40 nm) bilayer OPV cells.

Fig. 3(a), in which EQE was improved throughout the photo-response range. So the improvement is related to charge collection process. We did not see any changes in absorption of SQ films upon thermal annealing, and thus there is no thermal induced aggregation.²⁴ There is possibility that mixing of donor and acceptor at the interface due to the thermal treatment, and thus enhanced V_{oc} could also be expected.²⁵ Another possible reason could be the interface for hole collection. A thermal treatment may cause MoO₃ diffusion into SQ film, which improves anode contact with ITO substrates, and thus improves both charge collection and V_{oc} .²⁶

In spite of multiple possibilities, we tried to understand the issue based on the electric properties of the cells. From the dark J-V characteristics of fresh and annealed OPV cells in Fig 3(b), after thermal annealing, the current density under reversed bias decreased by one order of magnitude. Fitting J-V curves to the diode equation²⁷ yields significant difference in J_0 , as shown in Table I, while ideality factors (n) are close to 2. The fresh cell has J_0 of 8.13×10^{-8} mA/cm², and after annealing it is reduced to 3.04×10^{-8} mA/cm².

TABLE I. Photovoltaic performance of fresh and annealed SQ (9 nm)/C₇₀ (40 nm) bilayer device under 100 mW/cm² (AM 1.5 G solar spectrum).

Device	J_{sc} (mA/cm ²)	V_{oc} (V)	FF	PCE (%)	J_0 (mA/cm ²)
Fresh	7.3 ± 0.1	0.72 ± 0.01	0.58 ± 0.01	3.0 ± 0.2	8.13×10^{-8}
Annealed	7.8 ± 0.1	0.79 ± 0.01	0.63 ± 0.01	4.1 ± 0.2	3.04×10^{-8}

Considering the correlation between J_0 and V_{oc} , $V_{oc} = nkT/q \cdot \ln(J_{sc}/J_0)$, where k is the Boltzmann constant, T is the temperature, and q is the elemental charge, the reduction of J_0 should elevate V_{oc} by ~ 0.07 V, which matches our experimental observation. In inorganic semiconductor p-n junctions, J_0 measures thermal generation of charge carriers, representing the magnitude of charge recombination under thermal equilibrium.²⁸ Therefore, we believe the reduction of J_0 in our OPV cells indicates decrease of the recombination loss, which can be clearly seen in the improved shunt resistance and V_{oc} . Nevertheless, J_{sc} is merely improved by less 10% upon thermal treatment, and thus the optical simulation results still hold in annealed cells.

In conclusion, we investigated optical properties of SQ films via ellipsometry method. L_D of SQ was determined from numerical simulation and EQE data. Photovoltaic devices based on SQ/fullerene planar heterojunction were fabricated, achieving maximum PCE of 4.1%. Good agreement between the simulation results and experimental data was obtained, suggesting enormous potential of SQ and its analog compounds in organic photovoltaics.

We thank financial support from the Japan Science and Technology Agency (JST) via the Japan Regional Innovation Strategy Program by the Excellence (J-RISE), and Adaptable and Seamless Technology transfer Program (A-STEP, AS232Z00929D). We thank Dr. K. Nakayama, Dr. X. F. Wang, and Mr. Z. Q. Wang for technical assistance and scientific discussion.

¹C. W. Tang, *Appl. Phys. Lett.* **48**, 183 (1986).

²P. Peumans and S. R. Forrest, *Appl. Phys. Lett.* **79**, 126 (2001).

³B. Maennig, J. Drechsel, D. Gebeyehu, P. Simon, F. Kozlowski, A. Werner, F. Li, S. Grundmann, S. Sonntag, M. Koch, K. Leo, M. Pfeiffer, H. Hoppe, D. Meissner, N. S. Sariciftci, I. Riedel, V. Dyakonov, and J. Parisi, *Appl. Phys. A: Mater. Sci. Process.* **79**, 1 (2004).

⁴K. Schulze, C. Uhrich, R. Schüppel, K. Leo, M. Pfeiffer, E. Brier, E. Reinold, and P. Bäuerle, *Adv. Mater.* **18**, 2872 (2006).

⁵X. D. Dang, A. B. Tamayo, J. Seo, C. V. Hoven, B. Walker, and T. Q. Nguyen, *Adv. Funct. Mater.* **20**, 3314 (2010).

⁶Y. Liu, X. Wan, F. Wang, J. Zhou, G. Long, J. Tian, J. You, Y. Yang, and Y. Chen, *Adv. Energy Mater.* **1**, 771 (2011).

⁷Y. Sun, G. C. Welch, W. L. Leong, C. J. Takacs, G. C. Bazan, and A. J. Heeger, *Nature Mater.* **11**, 44 (2012).

⁸M. L. Zhang, H. Wang, H. K. Tian, Y. H. Geng, and C. W. Tang, *Adv. Mater.* **23**, 4960 (2011).

⁹B. Walker, C. Kim, and T. Q. Nguyen, *Chem. Mater.* **23**, 470 (2011).

¹⁰S. Y. Wang, E. I. Mayo, M. D. Perez, L. Griffe, G. D. Wei, P. I. Djurovich, S. R. Forrest, and M. E. Thompson, *Appl. Phys. Lett.* **94**, 233304 (2009).

¹¹G. D. Wei, S. Y. Wang, K. Sun, M. E. Thompson, and S. R. Forrest, *Adv. Energy Mater.* **1**, 184 (2011).

¹²G. Wei, X. Xiao, S. Wang, K. Sun, K. J. Bergemann, M. E. Thompson, and S. R. Forrest, *ACS Nano* **6**, 972 (2012).

¹³G. Chen, H. Sasabe, Z. Q. Wang, X. F. Wang, Z. R. Hong, Y. Yang, and J. Kido, *Adv. Mater.* **24**, 2768 (2012).

¹⁴M. Q. Tian, M. Furuki, I. Iwasa, Y. Sato, L. S. Pu, and S. Tatsuura, *J. Phys. Chem. B* **106**, 4370 (2002).

¹⁵V. Shrotriya, G. Li, Y. Yao, C. W. Chu, and Y. Yang, *Appl. Phys. Lett.* **88**, 073508 (2006).

¹⁶D. Yokoyama, A. Sakaguchi, M. Suzuki, and C. Adachi, *Org. Electron.* **10**, 127 (2009).

¹⁷L. A. A. Pettersson, L. S. Roman, and O. Inganäs, *J. Appl. Phys.* **86**, 487 (1999).

¹⁸D. Yokoyama, *J. Mater. Chem.* **21**, 19187 (2011).

¹⁹D. Yokoyama, Z. Wang, Y. Pu, K. Kobayashi, J. Kido, and Z. R. Hong, *Sol. Energy Mater. Sol. Cells* **98**, 472 (2012).

²⁰P. W. M. Blom, V. D. Mihailetschi, L. J. A. Koster, and D. E. Markov, *Adv. Mater.* **19**, 1551 (2007).

²¹D. Cheyns, B. P. Rand, and P. Heremans, *Appl. Phys. Lett.* **97**, 033301 (2010).

²²M. Hirade and C. Adachi, *Appl. Phys. Lett.* **99**, 153302 (2011).

²³J. Wagner, M. Gruber, A. Hinderhofer, A. Wilke, B. Bröker, J. Frisch, P. Amsalem, A. Vollmer, A. Opitz, N. Koch, F. Schreiber, and W. Brütting, *Adv. Funct. Mater.* **20**, 4295 (2010).

²⁴K. C. Deing, U. Mayerhöffer, F. Würthner, and K. Meerholz, *Phys. Chem. Chem. Phys.* **14**, 8328 (2012).

²⁵T. W. Ng, M. F. Lo, M. K. Fung, S. L. Lai, Z. T. Liu, C. S. Lee, and S. T. Lee, *Appl. Phys. Lett.* **95**, 203303 (2009); H. X. Wei, J. Li, Y. Cai, Z. Q. Xu, S. T. Lee, Y. Q. Li, and J. X. Tang, *Org. Electron.* **12**, 1422 (2011).

²⁶T. Matsushima and C. Adachi, *J. Appl. Phys.* **103**, 034501 (2008).

²⁷J. G. Xue, B. P. Rand, S. Uchida, and S. R. Forrest, *Adv. Mater.* **17**, 66 (2005)

²⁸J. L. Gray, *Handbook of Photovoltaic Science and Engineering*, 2nd ed., edited by A. Luque and S. Hegedus (Wiley, 2011), Chap. 3, p. 122.